



Cite this: DOI: 10.1039/c5tc00109a

Bromo induced reversible distinct color switching of a structurally simple donor–acceptor molecule by vapo, piezo and thermal stimuli†

Pachaiyappan Rajamalli, Parthasarathy Gandeepan, Min-Jie Huang and Chien-Hong Cheng*

Altering the luminescence properties of a material through external factors is an attractive feature that has the potential for various luminescence-related applications. Here, we report the synthesis and luminescence properties of two anthracene-based donor acceptor compounds, *N,N*-di-*p*-tolylanthracen-9-amine (**TAA**) and 10-bromo-*N,N*-di-*p*-tolylanthracen-9-amine (**TAAB**). In the solid state, the bromo-substituted compound **TAAB** shows reversible visible switching of the emission by external stimuli such as solvent, mechanical grinding and temperature. Single crystal X-ray studies, powder-XRD analysis and theoretical calculations reveal that switchable emission originated from the different stacking modes of **TAAB**. Furthermore, we have found that the bromo group interaction in the solid state plays a crucial role in this tunable emission. The other anthracene-based compound **TAA** does not show such switching of the emission by external stimuli. The observed changes in the luminescence of **TAAB** by external stimuli suggest potential applications in rewritable optical media, sensors, and optoelectronic devices.

Received 13th January 2015,
Accepted 9th February 2015

DOI: 10.1039/c5tc00109a

www.rsc.org/MaterialsC

1. Introduction

Stimuli-responsive organic luminescent materials are of great importance due to diverse applications such as sensors, security inks, memories, displays, switches and organic light emitting diodes.¹ Great efforts have been devoted to the molecular design and modification to achieve color tuning and luminescence properties.² Reversible switching of the luminescence properties of organic materials by controlling the molecular packing instead of chemical alteration is highly innovative and suitable for practical applications. Since the luminescence properties of organic solids greatly depend on the molecular packing and intermolecular interaction,³ control of the molecular orientation and stacking mode of fluorophores by external stimuli is an effective way to tune the luminescence properties of organic materials. In this regard, luminescent materials which exhibit dynamically switchable solid state emission properties, when they are subjected to external stimuli such

as light,⁴ mechanical force,⁵ vapour⁶ and temperature,⁷ have been reported.

In this context, the stimuli-responsive luminescent materials, donor (D)–acceptor (A) based systems, are highly desirable, if it can produce high-contrast fluorescence.^{8a–c} To date, anthracene-based stimuli-responsive D–A systems are rarely reported,^{8d–g} although anthracene derivatives are well-known luminescent materials, with wide applications in light-emitting devices.^{9a,b} Hydrogen bonding, π – π stacking and their collective interactions are important intermolecular interactions for the construction of stimuli supramolecular systems.^{9b–d} To explore a new system and a new mechanism for tunable luminescence by various external factors with reversibility is still a great challenge for practical applications. Our continued interest to find out new non-covalent interaction in the molecular packing and emission properties promotes us to undertake the current research.^{1f,h} Herein, we report the synthesis of a multi-stimuli responsive luminescent material, 10-bromo-*N,N*-di-*p*-tolylanthracen-9-amine (**TAAB**), its emission properties and crystal packing. This luminescent material responds sensitively to vapo, piezo and temperature stimuli reversibly with drastic color changes. More interestingly, intermolecular interactions of C and H with Br play a crucial role in the tunable emission properties. These non-covalent interactions are confirmed by single crystal-XRD.

Department of Chemistry, National Tsing Hua University, Hsinchu 30013, Taiwan.
E-mail: chcheng@mx.nthu.edu.tw; Fax: +886-3-572469; Tel: +886-3-5721454

† Electronic supplementary information (ESI) available: ¹H and ¹³C spectra of 10-bromo-*N,N*-di-*p*-tolylanthracen-9-amine, the single crystal structure, the photoluminescence spectrum and powder-XRD. CCDC 1017742 and 1017743. For ESI and crystallographic data in CIF or other electronic format see DOI: 10.1039/c5tc00109a

2. Results and discussion

2.1 Photophysical properties and solvatochromic effect

The structures of the molecules utilized in this study are shown in Fig. 1. *N,N*-di-*p*-tolylanthracen-9-amine (**TAA**) was synthesised in good yields from 9-bromoanthracene and ditolylamine using a palladium tri-*tert*-butylphosphine complex as the catalyst. Bromination of **TAA** by *N*-bromosuccinimide (NBS) gave the final product **TAAB** in good yield (Fig. 1).¹⁰

The detailed synthetic procedures and characterization data are given in the experimental section and ESI.† As depicted in Fig. S1 (ESI†), the absorptions of **TAA** and **TAAB** in different solvents are nearly the same ($\lambda_{\text{max}} \sim 440$ nm and 450 nm), but the emission of **TAA** shifts from 474 nm in *n*-hexane to 537 nm in DCM (Fig. 2a). Similarly the emission of **TAAB** shifts from 499 nm in *n*-hexane to 563 nm in DCM (Fig. 2b). The photographs of **TAA** and **TAAB** in various solvents under UV illumination are shown in Fig. 2c and d, respectively. The emission wavelengths strongly depend on the solvent used, revealing a bathochromic shift as the solvent polarity increases. Additionally, the fluorescence intensity is clearly reduced in highly polar solvents. These results indicate that the **TAAB** emission is likely a charge transfer type.

2.2 Theoretical calculations

To gain insight into the electronic states of these two compounds, density functionalized theory (DFT) calculations were performed using Gaussian 03 program. Fig. 3a shows the electron cloud of **TAA** and the result reveals that the highest occupied molecular orbital (HOMO) is mainly distributed on the electron donating tolylamine units and to a less extent on the anthracene group. On the other hand, the lowest unoccupied molecular orbital (LUMO) mostly spreads over the electron-accepting anthracene group. These results showed that **TAA** is a D–A dipole molecule with strong charge transfer properties from HOMO to LUMO in agreement with the observed solvent effect of the emission spectra. The HOMO and LUMO (Fig. 3b) of **TAAB** are similar to those of **TAA**. The HOMO is mainly distributed over the electron donating tolylamine unit and to a less extent on the bromoanthracene group and the LUMO mostly spreads over the electron-accepting bromoanthracene group.

2.3 Molecular packing controlled emission

As shown in Fig. 4b, **TAAB**, upon crystallization from *n*-hexane, appears as red material under ambient light with a yellow

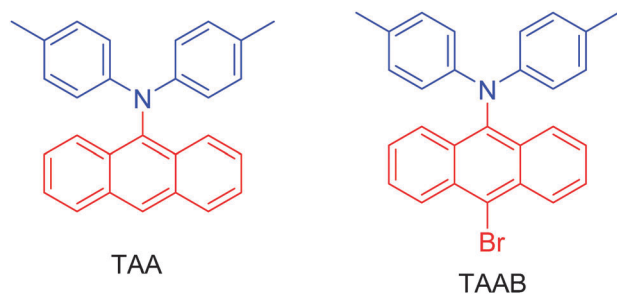


Fig. 1 Structures of **TAA** and **TAAB**.

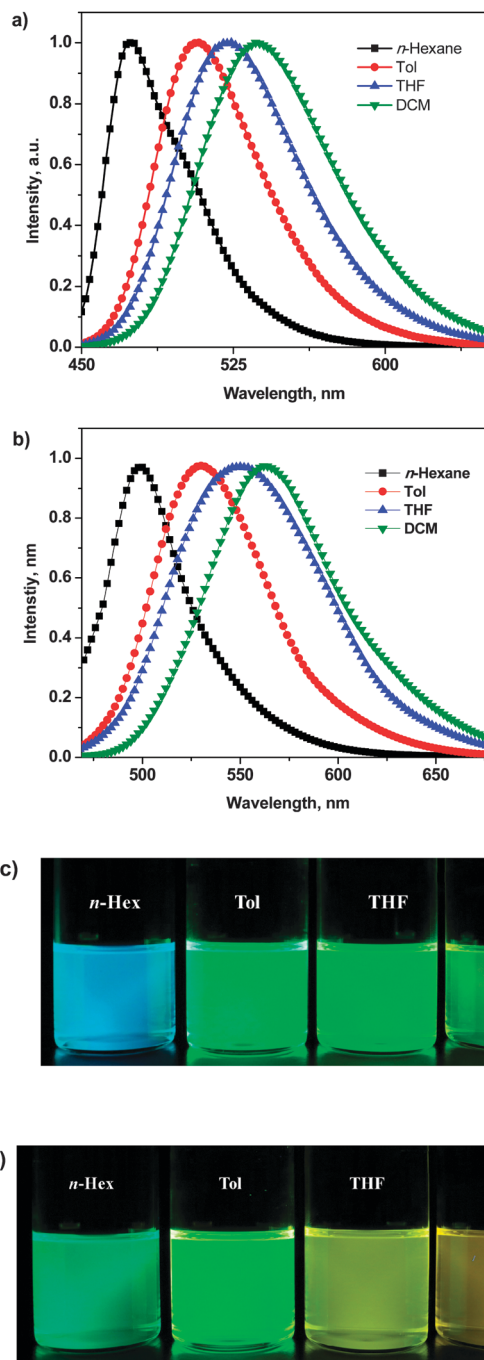


Fig. 2 Emission spectra of **TAA** (a) and **TAAB** (b) in various solvents at RT (10^{-5} M), and photographs of **TAA** (c) and **TAAB** (d) in various solvents under UV irradiation.

orange luminescence at 577 nm under UV radiation (Fig. 4d) in contrast to the emission at 499 nm in the same solution. On the other hand, when the compound was crystallized from DCM or exposed to DCM vapour, the crystals show a yellow color, giving green luminescence at 535 nm. A 42 nm hypsochromic shift from the yellow orange emission was observed (Fig. 4). Interestingly, the initial emission was recovered by heating the same at 70 °C. Such conversion between yellow orange and green emissions can be repeated many times

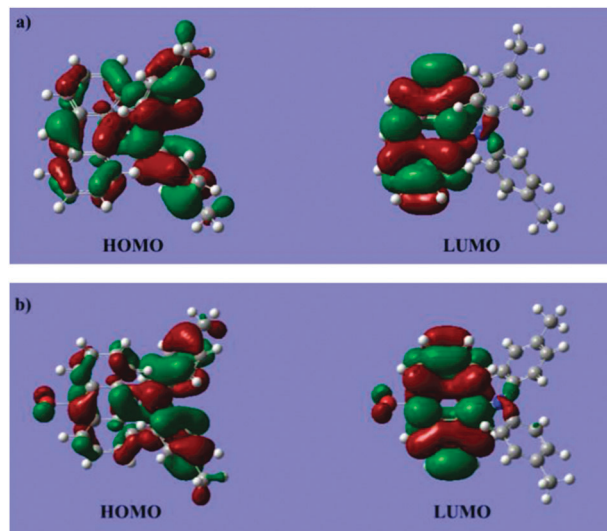


Fig. 3 Calculated electron contour plots (a) HOMO and LUMO molecular orbitals of **TAA**, and (b) HOMO and LUMO molecular orbitals of **TAAB**.

without decreasing the intensity plausibly due to the non-destructive nature of the solvent stimuli. It is worth noting that the solid-state stimuli properties were not observed for **TAA** suggesting that the Br group plays a crucial role in the tunable emission properties of **TAAB**. The luminescence properties of molecules in the solid state are known to be influenced by intermolecular interactions.¹¹ To understand the molecular packing and the intermolecular interactions of **TAAB**, single crystals grown from DCM and *n*-hexane were obtained by solvent evaporation. The crystalline structures were then determined by single-crystal X-ray diffraction analysis.

In *n*-hexane, **TAAB** was crystallized as monoclinic with each unit cell containing four **TAAB** molecules (Fig. S2, ESI†). On the other hand, in DCM, **TAAB** was crystallized as orthorhombic with each unit cell containing eight **TAAB** and 8 DCM molecules (Fig. S2, ESI†). The packings of **TAAB** crystals grown from different solvents are shown in Fig. 5. The crystals from *n*-hexane show that the molecules are lined up in a head-to-tail manner. As revealed in Fig. 5A, the Br group (head) interacts with the hydrogens and carbons on the two tolyl groups (tail) of the other molecule with interaction distances of 3.2–3.4 Å and 3.4–3.6 Å, respectively.

Since the Br group plays a crucial role in the emission properties, we performed the DFT calculations of two **TAAB** molecules with and without such interaction to see how strong this head to tail interaction is. The result shows that the interaction gives an energy decrease (stabilization) of 1.91 kcal mol^{−1} compared with the total energy of the two molecules without such interaction. The crystal packing further suggests there is no anthracene–anthracene interaction. However, the anthracene moieties show π – π and CH– π interactions with the tolyl groups of other molecules (Fig. 6). For the **TAAB**–DCM crystal, the anthracene groups are packed in a head-head manner. Each anthracene group overlaps with two other intermolecular anthracene groups *via* π – π stacking with the π -overlap

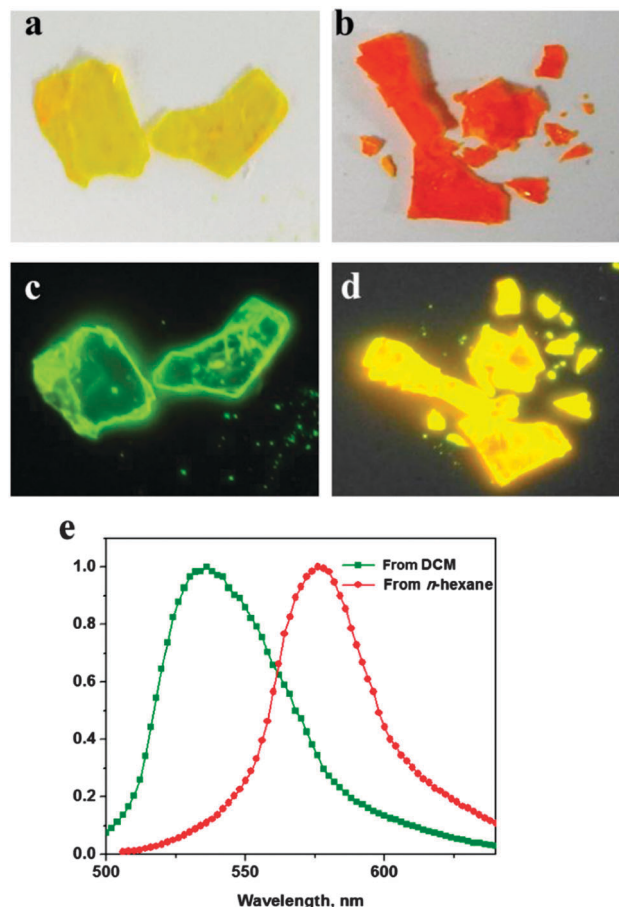


Fig. 4 Photographs of **TAAB** crystals: (a) crystallized from DCM and (b) from *n*-hexane under ambient light; (c) from DCM and (d) from *n*-hexane under UV-light; (e) fluorescence spectra of **TAAB** crystals from *n*-hexane (red line) and dichloromethane (green line).

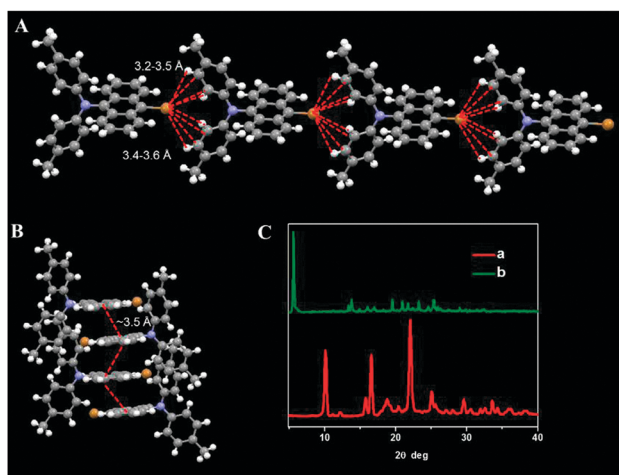


Fig. 5 Crystal packing of **TAAB**: (A) crystallized from *n*-hexane; (B) crystallized from DCM; (C) the corresponding PXRD patterns of **TAAB**: (a) crystallized from *n*-hexane and (b) crystallized from DCM.

area of about 1/4 (partial overlap) of an anthracene moiety and a distance of ~3.5 Å between the two overlapping anthracene planes.

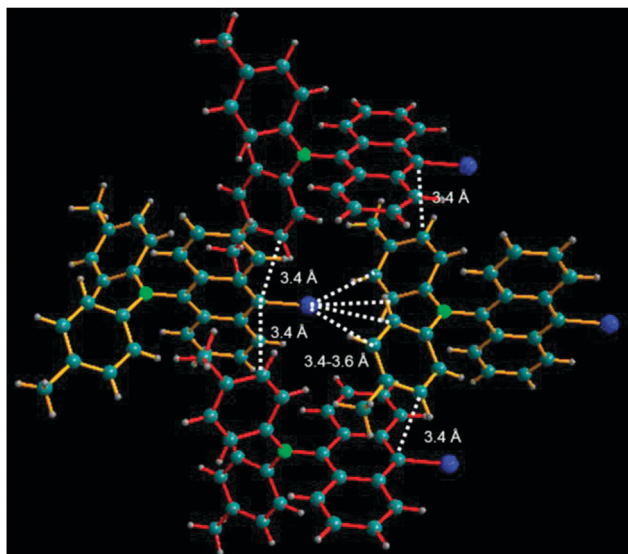


Fig. 6 Single crystal structure of **TAAB** crystallized from *n*-hexane (anthracene tolyl and Br–tolyl interaction).

We also performed the DFT calculations of two **TAAB** molecules with an anthracene–anthracene π – π interaction shown in Fig. 5B. A stabilization energy of 0.95 kcal mol^{−1} was found for the interaction of two anthracene groups. The stabilization energies due to the intermolecular interactions and the resultant HOMO and LUMO levels in the **TAAB** crystals likely account for the distinct colors and emission wavelengths, although the details need more studies. To further evaluate the relationship between the vapochromism and the structures, we measured the powder X-ray diffraction (PXRD) patterns of the **TAAB** crystallized from *n*-hexane and from DCM. As shown in Fig. 5C, different PXRD patterns were obtained for these two samples. The observed patterns are consistent with the simulated powder patterns from the single crystal X-ray analysis of **TAAB** and **TAAB**–DCM (Fig. S3, ESI†).

2.4 Tunable emission upon external pressure

It is interesting to mention that **TAAB** exhibits piezochromism of the crystalline sample. When the material was ground in a mortar by a pestle, drastic color change from orange red to yellow orange was found (Fig. 7). This property appears reversible as indicated by the heat treatment at 140 °C for 10 min of the ground sample. Its emission color reverts back to that of the unground sample (Fig. S4, ESI†). As indicated in Fig. 7, the emission maximum of **TAAB** at 577 nm was blue shifted to 543 nm after grinding. This is likely due to the fact that the intermolecular interactions (Fig. 5A and 6) were partially destroyed by the external pressure. It is noteworthy that grinding of crystals in many cases leads to red shift of the emission.¹² Conversely, **TAA** does not show a significant luminance change under external pressure and this result further confirms the importance of bromo interaction in piezochromism.

As shown in Fig. 5C-a, the PXRD pattern of **TAAB** shows intense and sharp peaks. In contrast, the ground sample of **TAAB** afforded very weak diffraction intensity (Fig. S5, ESI†).

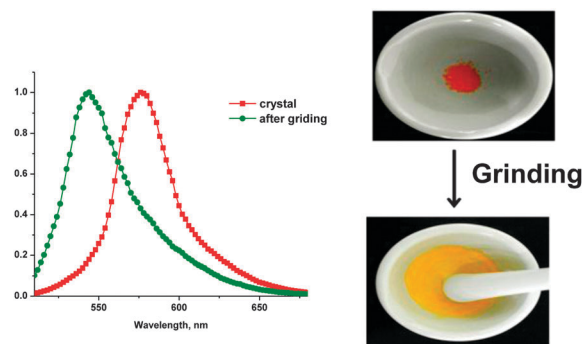


Fig. 7 (a) Normalized emission spectra of **TAAB** before and after grinding, (b) photographs of **TAAB** under ambient light before and after grinding.

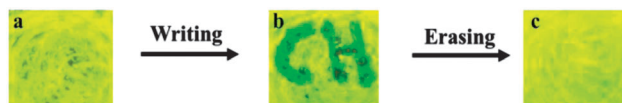


Fig. 8 Photoluminescence images of **TAAB** precipitated from *n*-hexane and ground in a mortar under UV irradiation at 365 nm. (a) A ground sample; (b) a sample after writing letters 'C' and 'H' with DCM solvent and (c) the same sample after erasing the letters by heating at 70 °C for 10 min and grinding.

The intensity decrease indicates that the grinding process converted the crystalline **TAAB** to an amorphous state.¹³ The observed small peaks in the PXRD pattern indicated that a small part of the crystalline sample remained after grinding. When the ground sample was heated at 140 °C for 10 min, the peaks in the PXRD pattern grew stronger. This result suggested that the amorphous ground sample could revert to the original crystalline state by heating. To demonstrate their utility for the practical application, a **TAAB** sample was taken into the mortar and was ground. The sample exhibited greenish-yellow emission under UV irradiation as shown in Fig. 8a. Letters 'C' and 'H' were written on the powder using DCM solvent to give green emission. The letters were erased upon heating the sample at 70 °C for 10 min and then grinding.

2.5 Temperature dependent fluorescence emission

Thermochromic photoluminescent materials in the solid state have received great attention due to the fact that photoluminescence is one of the most sensitive and easily detectable signals.^{7,14} However, in these cases, the thermochromism processes are sensitive to concentration and generally irreversible. Additionally, the fluorescent materials need to be doped into polymers along with a reference fluorescent material. To avoid these complications, a non-doped and highly luminescent material for the naked eye temperature indicator is highly desired. Here, we demonstrate that **TAAB** shows a reversible high contrast thermoresponsive luminescence. When **TAAB** was cooled to 77 K, the initial orange red material turns to a yellow solid under ambient light and the yellow-orange emission at 577 nm shifted to a bright greenish-yellow band at 542 nm under UV irradiation. As shown in Fig. 9, the color

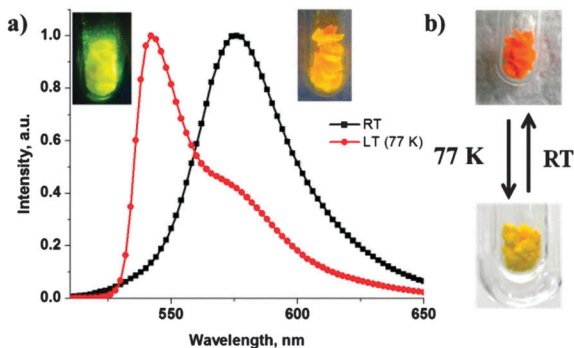


Fig. 9 (a) PL spectra of **TAAB** at RT and 77 K (insets: the corresponding photographs under UV light), (b) photographs at room temperature and 77 K under ambient light.

change is visible to the naked eye. The color change is reversible, and as the sample was warmed to room temperature, its color reverted back to orange red. This distinct reversible luminescence switching is very rarely observed in pure organic compounds in the solid state at low temperature.¹⁵ Further, to understand the sensitivity of the thermochromism, the time dependent fluorescence spectra were recorded at various time intervals at 77 K and room temperature and are shown in Fig. 10. The results suggest that fluorescence switching is fast when the crystals were cooled to 77 K or warmed to RT.

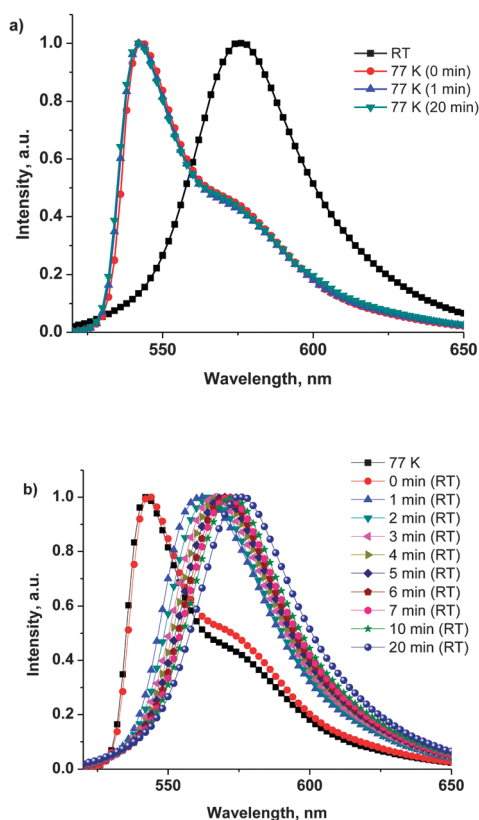


Fig. 10 Fluorescence spectra of **TAAB** crystals after (a) the crystals were cooled to 77 K; (b) the crystals at 77 K were warmed in the air to room temperature at various time intervals.

3. Conclusion

We have synthesized an anthracene-based D–A system **TAAB** which exhibits multi-stimuli responsive luminescence including solvent, piezo and thermochromism with a distinct color change. The crystalline sample of **TAAB** obtained from *n*-hexane exhibited interesting vapochromism behaviors with emission colors changing from yellow orange to green, upon exposure to DCM solvents. Single crystal analysis and theoretical calculations of the **TAAB**–DCM crystal indicated that the hypsochromic emission likely originated from the change in the molecular interaction of the **TAAB** molecules, change in Br-based interaction to anthracene-based one, leading to a larger energy gap. Furthermore, the emission color change was also observed upon grinding as well as cooling. It is noteworthy that this is the first example of a D–A compound which exhibits reversible multi-stimuli luminescence. The observed vapochromic, piezofluorochromic and thermochromic properties of this compound suggest potential applications in rewritable optical media, sensors, and optoelectronic devices. Comprehensive investigation in this direction is in progress in our laboratory.

4. Experimental section

4.1 General information

Reagents and solvents were used as purchased without further purification unless otherwise stated. ¹H and ¹³C NMR spectra were recorded using a Varian Mercury 400 spectrometer. The HRMS spectra were recorded on a Finnigan MAT-95XL mass spectrometer. UV-vis spectra were recorded on a Hitachi U-3300 spectrophotometer and PL spectra were measured using a Hitachi F-4500 fluorescence spectrophotometer. The molecular geometry optimizations and electronic properties were computed by carrying out the Gaussian 03 program with density functional theory (DFT) and time-dependent DFT (TDDFT) calculations, in which Becke's three-parameter functional combined with Lee, Yang, and Parr's correlation functional (B3LYP) and hybrid exchange–correlation functional with the 6-31G* basis set were used. The molecular orbitals were visualized on the Gaussview 4.1 software.

4.2 Synthesis of *N,N*-di-*p*-tolylanthracen-9-amine (TAA)

A mixture of 9-bromoanthracene (5.00 g, 19.6 mmol), Pd(OAc)₂ (43.0 mg, 0.19 mmol), tri-*tert*-butylphosphine (158.0 mg, 0.78 mmol), di-*p*-tolylamine (4.24 g, 21.6 mmol) and sodium *tert*-butoxide (3.10 g, 32 mmol) in dry *o*-xylene (40 mL) was placed in a sealed tube under a nitrogen atmosphere and was stirred at 120 °C for 15 h. After cooling, water was added to the reaction mixture and the mixture was then extracted with ethyl acetate. The organic layer was dried over anhydrous MgSO₄ and evaporated under vacuum. The crude product was purified by silica gel column chromatography eluted with *n*-hexane to give the desired yellow solid in 89% yield. ¹H NMR (400 MHz, CDCl₃): δ 8.45 (s, 1H), 8.09 (d, 2H, *J* = 8.8 Hz), 8.02 (d, 2H, *J* = 8.4 Hz), 7.33–7.43 (m, 4H), 6.92 (s, 8H), 2.20 (s, 6H); ¹³C NMR (100 MHz, CDCl₃): δ 145.8, 137.8, 133.1, 131.04, 130.4, 129.9,

129.2, 126.8, 125.7, 124.8, 124.7, 120.3, 20.9; HRMS (EI^+) calcd for $\text{C}_{28}\text{H}_{23}\text{N}$ 373.1830, found 373.1833; IR (KBr): 3025, 2919, 2859, 1608, 1506, 1440, 1407, 1355, 1315, 1292, 811 and 734 cm^{-1} .

4.3 Synthesis of 10-bromo-*N,N*-di-*p*-tolylanthracen-9-amine (TAAB)

TAA (5.00 g, 134 mmol) and *N*-bromosuccinimide (NBS) (2.86 g, 161 mmol) were dissolved in DMF:CHCl₃ (1 : 3, 60 mL) and the solution was stirred at room temperature for 6 h. After completion of reaction, water was added to the reaction mixture and the mixture was extracted with dichloromethane. The organic layer was dried over anhydrous MgSO₄ and evaporated under vacuum. The product was purified by silica gel column chromatography eluted with *n*-hexane. Red crystals of **TAAB** were obtained in 86% yield. ¹H NMR (400 MHz, CDCl₃): δ 8.57 (d, 2H, $J = 8.4\text{ Hz}$), 8.13 (d, 2H, $J = 8.4\text{ Hz}$), 7.37–7.56 (m, 4H), 6.89–6.94 (m, 8H), 2.21 (s, 6H); ¹³C NMR (100 MHz, CDCl₃): δ 145.2, 138.1, 131.6, 131.5, 130.5, 129.7, 128.4, 127.2, 126.9, 124.9, 122.3, 120.0, 20.6; HRMS (EI^+) calcd for $\text{C}_{28}\text{H}_{22}\text{BrN}$ 451.0936, found 451.0935; IR (KBr): 3025, 2919, 2854, 1608, 1504, 1436, 1405, 1353, 1315, 1292, 809, 755 and 734 cm^{-1} .

Acknowledgements

We thank Ministry of Science and Technology of Republic of China (MOST 103-2633-M-007-001) for support of this research.

Notes and references

- (a) M. Irie, T. Fukaminato, T. Sasaki, N. Tamai and T. Kawai, *Nature*, 2002, **420**, 759; (b) S. S. Babu, K. K. Kartha and A. Ajayaghosh, *J. Phys. Chem. Lett.*, 2010, **1**, 3413; (c) Y. Sagara and T. Kato, *Nat. Chem.*, 2009, **1**, 605; (d) T. Mutai, H. Satou and K. Araki, *Nat. Mater.*, 2005, **4**, 685; (e) X.-d. Wang, O. S. Wolfbeis and R. J. Meier, *Chem. Soc. Rev.*, 2013, **42**, 7834; (f) P. Rajamalli and E. Prasad, *Soft Matter*, 2012, **8**, 8896; (g) A. Ajayaghosh, V. K. Praveen, S. Srinivasan and R. Varghese, *Adv. Mater.*, 2007, **19**, 411; (h) P. Rajamalli and E. Prasad, *Org. Lett.*, 2011, **13**, 3714; (i) P. Rajamalli and E. Prasad, *New J. Chem.*, 2011, **35**, 1541; (j) A. Ajayaghosh, V. K. Praveen, C. Vijayakumar and S. J. George, *Angew. Chem.*, 2007, **119**, 6376; (k) S.-J. Yoon, S. Varghese, S. K. Park, R. Wannemacher, J. Gierschner and S. Y. Park, *Adv. Opt. Mater.*, 2013, **1**, 232; (l) K. K. Kartha, S. S. Babu, S. Srinivasan and A. Ajayaghosh, *J. Am. Chem. Soc.*, 2012, **134**, 4834; (m) S. S. Babu, V. K. Praveen and A. Ajayaghosh, *Chem. Rev.*, 2014, **114**, 1973; (n) K. K. Kartha, A. Sandeep, V. C. Nair, M. Takeuchi and A. Ajayaghosh, *Phys. Chem. Chem. Phys.*, 2014, **16**, 18896.
- (a) Z. Zhang, B. Xu, J. Su, L. Shen, Y. Xie and H. Tian, *Angew. Chem., Int. Ed.*, 2011, **50**, 11654; (b) Z. Zhao, Z. Wang, P. Lu, C. Y. K. Chan, D. Liu, J. W. Y. Lam, H. H. Y. Sung, I. D. Williams, Y. Ma and B. Z. Tang, *Angew. Chem., Int. Ed.*, 2009, **48**, 7608; (c) R. Davis, N. S. S. Kumar, S. Abraham, C. H. Suresh, N. P. Rath, N. Tamaoki and S. Das, *J. Phys. Chem. C*, 2008, **112**, 2137; (d) H. Y. Zhang, Z. L. Zhang, K. Q. Ye, J. Y. Zhang and Y. Wang, *Adv. Mater.*, 2006, **18**, 2369; (e) C.-H. Chen, F.-I. Wu, Y.-Y. Tsai and C.-H. Cheng, *Adv. Funct. Mater.*, 2011, **21**, 3150; (f) Y. Dong, B. Xu, J. Zhang, X. Tan, L. Wang, J. Chen, H. Lv, S. Wen, B. Li, L. Ye, B. Zou and W. Tian, *Angew. Chem., Int. Ed.*, 2012, **51**, 10782.
- (a) S. J. Yoon, J. W. Chung, J. Gierschner, K. S. Kim, M. G. Choi, D. Kim and S. Y. Park, *J. Am. Chem. Soc.*, 2010, **132**, 13675; (b) E. Takahashi, H. Takaya and T. Naota, *Chem. – Eur. J.*, 2010, **16**, 4793; (c) S. P. Anthony, *ChemPlusChem*, 2012, **77**, 518; (d) S. P. Anthony, S. Varughese and S. M. Draper, *Chem. Commun.*, 2009, 7500; (e) T. Mutai, H. Tomoda, T. Ohkawa, Y. Yabe and K. Araki, *Angew. Chem., Int. Ed.*, 2008, **47**, 9522; (f) A. L. Balch, *Angew. Chem., Int. Ed.*, 2009, **48**, 2641.
- (a) Special edition: Photochromism: Memories and Switches, ed. M. Irie, *Chem. Rev.*, 2000, **100**; (b) K. Li, Y. Xiang, X. Wang, J. Li, R. Hu, A. Tong and B. Z. Tang, *J. Am. Chem. Soc.*, 2014, **136**, 1643.
- Z. Ma, M. Teng, Z. Wang, S. Yang and X. Jia, *Angew. Chem., Int. Ed.*, 2013, **52**, 12268.
- T. Nishiuchi, K. Tanaka, Y. Kuwatani, J. Sung, T. Nishinaga, D. Kim and M. Iyoda, *Chem. – Eur. J.*, 2013, **19**, 4110.
- J. Feng, L. Xiong, S. Wang, S. Li, Y. Li and G. Yang, *Adv. Funct. Mater.*, 2013, **23**, 340.
- (a) Y. Zhang, J. Sun, G. Zhuang, M. Ouyang, Z. Yu, F. Cao, G. Pan, P. Tang, C. Zhang and Y. Ma, *J. Mater. Chem. C*, 2014, **2**, 195; (b) J. Luo, L. Y. Li, Y. L. Song and J. Pei, *Chem. – Eur. J.*, 2011, **17**, 10515; (c) Z.-H. Guo, Z.-X. Jin, J.-Y. Wang and J. Pei, *Chem. Commun.*, 2014, **50**, 6088; (d) S. S. Babu, M. J. Hollamby, J. Aimi, H. Ozawa, A. Saeki, S. Seki, K. Kobayashi, K. Hagiwara, M. Yoshizawa, H. Moehwald and T. Nakanishi, *Nat. Commun.*, 2013, **4**, 1969; (e) M. Yoshizawa and J. K. Klosterman, *Chem. Soc. Rev.*, 2014, **43**, 1885; (f) Z. Zhang, D. Yao, T. Zhou, H. Zhang and Y. Wang, *Chem. Commun.*, 2011, **47**, 7782; (g) X. Zhang, Z. Chi, X. Zhou, S. Liu, Y. Zhang and J. Xu, *J. Phys. Chem. C*, 2012, **116**, 23629.
- (a) J. Zhang, J. Chen, B. Xu, L. Wang, S. Ma, Y. Dong, B. Li, L. Ye and W. Tian, *Chem. Commun.*, 2013, **49**, 3878; (b) H. Zhang, Z. Zhang, K. Ye, J. Zhang and Y. Wang, *Adv. Mater.*, 2006, **18**, 2369; (c) Y. Dong, J. Zhang, X. Tan, L. Wang, J. Chen, B. Li, L. Ye, B. Xu, B. Zou and W. Tian, *J. Mater. Chem. C*, 2013, **1**, 7554; (d) Y. Sagara, T. Mutai, I. Yoshikawa and K. Araki, *J. Am. Chem. Soc.*, 2007, **129**, 1520.
- (a) M.-X. Yu, X.-H. Chen and C.-H. Cheng, *Chin. J. Org. Chem.*, 2005, **25**, 218; (b) M.-X. Yu, J.-P. Duan, C.-H. Lin, C.-H. Cheng and Y.-T. Tao, *Chem. Mater.*, 2002, **14**, 3958.
- J. Cornil, D. Beljonne, J. P. Calbert and J. L. Brédas, *Adv. Mater.*, 2001, **13**, 1053.
- (a) Z. Zhang, D. Yao, T. Zhou, H. Zhang and Y. Wang, *Chem. Commun.*, 2011, **47**, 7782; (b) P. Xue, B. Yao, X. Liu, J. Sun, P. Gong, Z. Zhang, C. Qian, Y. Zhang and R. Lu, *J. Mater. Chem. C*, 2015, **3**, 1018; (c) M. Zheng, D. T. Zhang, M. X. Sun,

- Y. P. Li, T. L. Liu, S. F. Xue and W. J. Yang, *J. Mater. Chem. C*, 2014, **2**, 1913.
- 13 (a) Z. Zhang, D. Yao, T. Zhou, H. Zhang and Y. Wang, *Chem. Commun.*, 2011, **47**, 7782; (b) Y. Gong, Y. Tan, J. Liu, P. Lu, C. Feng, W. Z. Yuan, Y. Lu, J. Z. Sun, G. He and Y. Zhang, *Chem. Commun.*, 2013, **49**, 4009; (c) M. S. Kwon, J. Gierschner, S.-J. Yoon and S. Y. Park, *Adv. Mater.*, 2012, **24**, 5487.
- 14 (a) L. H. Fischer, G. S. Harms and O. S. Wolfbeis, *Angew. Chem., Int. Ed.*, 2011, **50**, 4546; (b) F. Hammerer, G. Garcia, P. Charles, A. Sourdon, S. Achelle, M.-P. Teulade-Fichou and P. Maillard, *Chem. Commun.*, 2014, **50**, 9529; (c) R. Tian, R. Liang, D. Yan, W. Shi, X. Yu, M. Wei, L. S. Li, D. G. Evans and X. Duan, *J. Mater. Chem. C*, 2013, **1**, 5654; (d) X.-d. Wang, O. S. Wolfbeis and R. J. Meier, *Chem. Soc. Rev.*, 2013, **42**, 7834; (e) Y. Zhao, H. Gao, Y. Fan, T. Zhou, Z. Su, Y. Liu and Y. Wang, *Adv. Mater.*, 2009, **21**, 3165.
- 15 X. Liu, S. Li, J. Feng, Y. Li and G. Yang, *Chem. Commun.*, 2014, **50**, 2778.